EVOLUTION OF THE STRATOSPHERIC TEMPERATURE AND CHEMICAL COMPOSITION OVER ONE TITANIAN YEAR

ATHENA COUSTENIS[1], G. BAMPASIDIS[1,2], R. K. ACHTERBERG[3,4], P. LAVVAS[5], D. E. JENNINGS[3], C. A. NIXON[3], N. A. TEANBY[6], S. VINATIER[1], F. M. FLASAR[3], R. C. CARLSON[3,7], G. ORTON[8], P. N. ROMANI[3], E. A. GUANDIQUE[3,9], S. STAMOGIORGOS[2,10].

[1]Laboratoire d'Etudes Spatiales et d'Instrumentation en Astrophysique (LESIA), Observatoire de Paris, CNRS, UPMC Univ. Paris 06, Univ. Paris-Diderot, 5, place Jules Janssen, 92195 Meudon Cedex, France; athena.coustenis@obspm.fr

[2]Faculty of Physics, National and Kapodistrian University of Athens, Panepistimioupolis, GR 15783 Zographos, Athens, Greece

[3]NASA/Goddard Space Flight Center, Greenbelt, MD 20771, USA

[4]Department of Astronomy, University of Maryland, College Park, MD 20742, USA

[5]GSMA, Université Reims Champagne-Ardenne, France

[6]School of Earth Sciences, University of Bristol, Bristol, BS8 1RJ, UK

[7]IACS, Catholic University of America, USA

[8]MS 183-501, Jet Propulsion Laboratory, California Institute of Technology, 4800 Oak Grove Drive, Pasadena, California 91109, USA

[9]Adnet Systems, Inc., Rockville, MD, USA

[10]Technische Universität München (TUM) Germany

Submitted to The Astrophys. Journal Letters
4 September 2013

Running Head: Temporal variations in Titan's stratosphere since Voyager

ABSTRACT

Since the Voyager 1 (V1) flyby in 1980, Titan's exploration from space and the ground has been on-going for more than a full revolution of Saturn around the Sun (one Titan year or 29.5 Earth years was completed in May 2010). In this study we search for temporal variations affecting Titan's atmospheric thermal and chemical structure within that year. We process Cassini/CIRS data taken during the Titan flybys from 2006-2013 and compare them to the 1980 V1/IRIS spectra (re-analyzed here). We also consider data from Earth-based and -orbiting observatories (such as from the ISO, re-visited). When we compare the CIRS 2010 and the IRIS data we find limited inter-annual variations, below the 25% or 35% levels for the lower and middle, or the high latitudes, respectively. A return to the 1980 stratospheric temperatures and abundances is generally achieved from 50°N to 50°S, indicative of the solar radiation being the dominating energy source at 10 AU, as for the Earth, as predicted by GCM and photochemical models. However, some exceptions exist among the most complex hydrocarbons (C_4H_2 and C_3H_4), especially in the North. In the Southern latitudes, since 2012, we see a trend for an increase of several trace gases, possibly indicative of a seasonal atmospheric reversal. At the Northern latitudes we found enhanced abundances around the period of the northern spring equinox in mid-2009 (as in Bampasidis et al. 2012), which subsequently decreased (from 2010-2012) returning to values similar to those found in the V1 epoch a Titanian year before.

Key words: infrared: solar system - planets and satellites: individual (Titan) - atmospheres - planets and satellites: composition - radiation mechanisms: thermal - radiative transfer

1. INTRODUCTION

Mid-2010 Cassini observations marked one Titan year since the first extended space exploration of the satellite by Voyager 1 (V1) during the 12 November 1980 flyby. Titan, Saturn's largest moon, follows its planet on its course around the Sun on an inclined orbit (26.7°) which gives rise to seasons, similarly to Earth. The Cassini mission had performed 68 Titan flybys by May 2010 (See Tables 1-4 in Bampasidis et al. 2012) when the 9° solar longitude (Ls), was almost exactly the same as at the time of the V1 flyby (just after spring equinox in the northern hemisphere). Since then, and until the end of 2012, more mid-infrared nadir spectra of Titan were acquired, which we analyze here. These data allow us to probe Saturn's and, especially in what concerns us here, Titan's stratosphere (i.e. altitudes between ~100 and 500 km above the surface), where neutral species include hydrocarbons, nitriles and oxygen compounds.

Stratospheric temperatures and the trace gaseous content, as well as the associated vertical and meridional (latitudinal) distributions, have been reported both from Voyager and Cassini data (Coustenis and Bézard 1995; Achterberg et al. 2008, 2011; Coustenis et al. 1991, 2007, 2010; Teanby et al. 2008, 2009, 2012; Vinatier et al. 2007, 2010a,b). Here we search for temporal variations within these structures in Titan's stratosphere. Such an investigation was first performed between the two Titan Voyager 1 and 2 thermal IR datasets (Letourneur and Coustenis 1993) just months apart (the results were quite similar within error bars). Since then, other investigators have reported seasonal variations and trends during the Cassini mission (e. g. Teanby et al. 2008, 2009, 2010, 2012; Jennings et al. 2012; Bampasidis et al. 2012).

2. OBSERVATIONS

The V1/IRIS instrument, a Michelson interferometer that covered the 180-1500 cm^{-1} range (Hanel et al. 1980; Flasar et al. 2004), acquired about 300 usable spectra with a resolution of 4.3 cm^{-1} during the 1980 Titan flyby. Its heir, the Composite Infrared Spectrometer (CIRS), acquired a large number of spectra during the Cassini Titan flybys (about 90 by the end of 2012), in the thermal infrared range from 600 to 1430 cm^{-1} (focal plane 3, or FP3 (600-1100 cm^{-1}), and 4 or FP4 (1100-1430 cm^{-1}) in nadir and limb geometry conditions at high, medium and low spectral resolutions (0.53, 2.54 and 15

cm^{-1} respectively; Flasar et al. 2005). The CIRS data represent a significant improvement in number of spectra, spatial coverage, data quality and spectral resolution (by about an order of magnitude, see Figure 1).

We analyze several averages of CIRS nadir-viewing FP3 and FP4 spectra at medium and high resolution during the Cassini mission from July 2004 until 2013, complementing our previous analysis, which stopped in 2010 at flyby T72 (Bampasidis et al., 2012), by including data from 2011 and 2012 Cassini/CIRS spectra at 50°N, 50°S and near-equator. In particular, we have added one selection for 50°N recorded in September 2012 (T86 flyby) with 761 spectra (35.5 S/N and 1.24 airmass) in FP3 and 831 spectra (57.6 S/N and 1.28 airmass) in the associated FP4. Similarly, for 50°S a selection from September 2012 contains 777 spectra (22.5 S/N and 1.34 airmass) in FP3 and 612 spectra (30.4 S/N and 1.27 airmass) in FP4. At the equatorial latitudes, we have included three more selections recorded in January, February and May 2012 during the T81, T82 and T83 Cassini flybys respectively, with 1431, 1147 and 617 spectra for each FP3 (S/N : 57.7, 53.3 and 34.5 ; airmass :1.19, 1.01 and 1.01, respectively). In the FP4 region we have 1469, 1131 and 551 spectra for each flyby with S/N of 129.5, 116.5 and 79.9 and 1.10, 1.11 and 1.01 airmasses, respectively.

We have also compiled a listing of stratospheric-pertaining ground-based and Infrared Space Observatory (ISO, Coustenis et al. 2003) abundance inferences. These values are not disk-resolved and some times refer to different levels in the atmosphere of Titan, so that direct comparisons are difficult with the space data, all the more so since the error bars are not firmly defined in most of the ground-based studies. These refer mostly to molecules such as C_2H_6 and HCN (Table 1, *machine readable*) and the snapshots we have between 1980 and the Cassini mission show no large departures from one season to the other for these few molecules. The data from ISO/SWS taken in 1997 concern more molecules and are briefly discussed hereafter, where we mainly focus on comparisons between CIRS and IRIS, as these space datasets are the most directly comparable.

3. ANALYSIS

In this work we use Cassini/CIRS data to extend the 2006-2010 study of Bampasidis et al. (2012) until the end of 2012. We combine this with a re-analysis of the Voyager data and ISO datasets in order to define the neutral chemistry and atmospheric evolution on Titan on timescales longer than a Titan year. We focus on latitudes from 50°S to 50°N as these have the most complete temporal coverage.

We use our radiative-transfer code ARTT (Coustenis et al. 2010; Bampasidis et al. 2012), which includes several new molecules and the updated spectroscopic parameters for the gases and their isotopologues (Coustenis et al. 2003, 2008; Jennings et al. 2008; Nixon et al. 2008a,b, 2009; Rothman et al. 2009; Jacquinet-Husson et al. 2011). The thermal structure is derived using an *a priori* approach described in Achterberg et al. (2008, 2011) and applied on the Cassini/CIRS and V1/IRIS data by fitting the ν_4 methane band at 1305 cm^{-1} (Figure 1). The altitude/pressure ranges probed by the temperature profiles depend on the latitude, but are in general between 0.1 and 10 mbar (for details see Coustenis et al. 1995, 2003, 2010; Bampasidis et al., 2012). We then use the temperature profile in our radiative transfer code to derive the chemical composition of the trace gases in the rest of the spectrum.

We apply this method to different latitudes from 50°N to 50°N for CIRS and IRIS. The mixing ratios are assumed to be vertically-constant profiles above the condensation level and the altitudes probed for all space data correspond in general essentially to 100-250 km (0.5-10 mbar, see Coustenis et al. 2010 and Bampasidis et al. 2012 for more details). When the C_2H_2 band is not properly fitted at high or low resolution in the entire range with such a profile, we give an averaged abundance over the 700-750 cm^{-1} range in the results (for details see Coustenis et al. 1995, 2010). The contribution functions for these molecules remain within the ranges determined in these previous papers.

Our comparison with V1/IRIS date is restrained to those molecules with strong enough emission bands to be unambiguously detected also in the Voyager spectra with high enough S/N ratio and sufficient accuracy. These molecules are: CO_2, HCN, C_2H_2, C_2H_6, C_3H_4, C_4H_2. In this analysis we do not include the results we infer for C_3H_8 and C_2H_4, which suffer from higher uncertainty than the other molecules, since their weak and/or blended bands are difficult to exploit in the V1/IRIS spectra.

Table 2 shows the re-analyses of the V1/IRIS data (updating Coustenis and Bézard 1995) and of the ISO Short Wavelength Spectrometer (SWS) disk-averaged spectrum (updating Coustenis et al. 2003) using the same model as for the CIRS data. The differences with the previous publications are minor, except for the molecules that benefited from significantly improved spectroscopic parameters.

4. RESULTS ON THE STRATOSPHERIC STRUCTURE DURING ONE TITANIAN YEAR

The best fits obtained for the V1/IRIS and the January 2010 Cassini/CIRS 50°N selections are shown in Figure 1.

4.1 *Inter-annual temperature variations*

We compare the new temperature profiles inferred for the Voyager selections with the ones found for 2010 from CIRS data at 50°N, equator and 50°S (Fig. 2). We also overplot on that figure the temperature profile that corresponds to the disk-average ISO observations of 1997, which pertain morst closely to conditions at mid-latitudes.

In the southern hemisphere, the 1980 and 2010 temperature profiles are quite similar, with very small differences of less than 5 K and more typically 2-3 K between 0.1 (250 km) and 10 mbar (100 km), in the region probed by our data. Above the 0.1-mbar pressure level the temperature appears to be cooling, e.g., by as much as 15 K at 0.01 mbar (400 km) from 2005 to 2010, but these inferences are very uncertain because the nadir data do not probe such high altitudes. The reader is referred to limb-data analyses as, for instance, in Vinatier et al. (2007, 2010) for the temperatures at higher altitudes. The revised Voyager temperature profiles are then consistent with the CIRS 2010 ones in the lower latitudes and no significant variations are detected.

Similarly, no significant change was found in the equatorial mid-stratospheric temperatures, with the 1980 and the 2010 temperature profiles always within 5-6 K of each other up to the 0.1-mbar level, although again it appears that a cooler equatorial mesosphere is observed after one Titan year as in the South. We note that the temperature profile corresponding to the ISO 1997 data follows very closely the CIRS 2010 profile throughout the equatorial stratosphere. All in all, the average vertical stratospheric temperature profiles from 50°S to the equator appear quite to each other at all times. The 50°S temperatures are about 3-6 K cooler than the equatorial ones for CIRS (see e. g. Bampasidis et al. 2012 for more precise information on the thermal evolution during the Cassini mission).

At northern latitudes, temporal variations were reported during the Cassini mission, while the shape of the thermal structure changed towards a vertically more homogeneous profile in the past 4 years not showing the marked stratopause observed earlier (Achterberg et al. 2011, Bampasidis et al. 2012). However, when we compare the 1980 and the 2010 stratospheric profiles at 50°N, we find the V1 profile to be quite compatible to the CIRS one, equivalent within 3-4 K up to the 0.2-mbar (220 km) level. Thus, in the stratosphere, the thermal structure has returned to the V1 shape after a Titanian year (Fig. 2).

4.2 *Chemical composition variations*

With the temperature profiles determined as indicated above, we infer the chemical composition for Titan's stratosphere from CIRS, IRIS and ISO spectra. The new and more accurate chemical composition inferred at the time of the Voyager 1 encounter (12 Nov. 1980) is given in Table 2 for the latitudes of interest here. The revised abundances for the ISO/SWS data of 1997 are also listed in that Table.

The ratios of the CIRS calculations (of high resolution, 0.5 cm^{-1}) with respect to the V1/IRIS values (dividing each CIRS result with the V1/IRIS 1980 inference) are shown in Fig. 3 for 50°S, equator, and 50°N. Since the model parameters for all these calculations are the same, we only consider the relative uncertainties that are generally small for the CIRS data (since the noise is small, given the large number of spectra summed) but mainly concern uncertainties as to some of the spectroscopic data and temperature profile inferences (see Bampasidis et al. 2012 for details). In Fig. 3 we display only these relative error bars for all the molecules so that we can derive the variations with time within the Cassini mission period for each species. Note that the ratios are not indicative of any variations wrt to V1/IRIS except for the 2010 period, when they are meaningful. Indeed, for the time when we return to the V1 epoch, one needs to consider in addition, when comparing CIRS and IRIS, the uncertainty due to the V1/IRIS random errors (noise, calibration, temperature profile determination and fit of the continuum). When this is taken into account, at the 2010 dates indicated by arrows in Fig. 3, the level of uncertainty on the ratio (total between the IRIS and the CIRS error bars) is 27%, 23% and 35% for 50°S, equator and 50°N, respectively.

Hereafter we compare for each molecule: a) the trend during the Cassini mission shown by the ratios; b) the comparison with the abundances a Titan year ago, around mid-2010.

4.2.1 Seasonal evolution of the stratospheric composition

Starting with the lower latitudes (50°S), we find that during the Cassini mission, the CIRS high-resolution data indicate that, within measurement uncertainties, CO_2, C_2H_2 and C_2H_6 can be considered unvarying to within 25% up to 2013, as indicated also in Bampasidis et al (2012), while HCN, C_4H_2 and C_3H_4 show some excursions, especially in the more recent years (Fig. 3a). We further note that the results from the analysis of the Sept. 2012 selection indicate that there is a significant increase of the abundances of some of the molecules like C_4H_2, C_3H_4, CO_2, and HCN, while other more abundant molecules (C_2H_2 and C_2H_6) remain constant. This increase in abundance is compatible with the expected seasonal reversal in Titan’s stratospheric composition for some gases and the haze (see Teanby et al. 2012; Jennings et al., 2012 and references therein).

Fig. 3b shows the situation for the equator during the Cassini mission and until 2013, in which we find, as for 50°S, rather constant variations with time for all molecules. C_4H_2 appears to have decreased in abundance from 2008 to 2012 by 30%, but the abundance of this molecule suffers of large uncertainties due to its lacking spectroscopic parameters. Since 2011, the concentrations of all the gases show a trend for a certain decrease, which will need further confirmation.

As noted in Bampasidis et al (2012), at 50°N, we also find that, with the possible exception of C_2H_6, CO_2 and C_3H_4, all the molecules show significant variations with time during the Cassini mission. Thus, while from 2007 to mid-2008 the gas mixing ratios are constant to within 30%, we detect a general trend for a pronounced increase from mid-2008 to mid-2009 with a maximum (by factors of 2-3) for almost all molecules in April-May 2009 (the closest to Titan's northern spring equinox, NSE, August 2009). This is followed by a strong decrease, which reduces the 2010 concentrations to the values of the period preceding the increase (Fig. 3c), as confirmed by the Sept. 2012 data.

4.2.2 Inter-annual compositional variations

We compare CIRS 2010 abundances with the retrievals of the V1/IRIS (1980) re-analyses by computing the ratios for the observed molecules. For comparison's sake with the V1/IRIS data, we have included some abundance retrievals from medium-resolution (2.5 cm^{-1}) CIRS spectra for 2010. The arrows in Fig. 3 point to the V1 encounter.

At 50°S, the 2010 April high-resolution and May-June medium-resolution spectra are very compatible with each other. However, the abundances derived from the medium-resolution spectra are generally slightly higher by 10-15% (Fig. 3a). All gaseous abundances from the CIRS datasets are within ±25-30% of the values observed in 1980 by Voyager 1 for both the higher and lower resolution measurements, which, given the difference in resolution and attitudes probed, can be considered as quite compatible. Exceptions are the more complex hydrocarbons (C_3H_4 and C_4H_2), which are below the V1/IRIS abundances at about 30-40% (Fig. 3a).

The 2010 equatorial CIRS mixing ratios of all the species from all resolution data are within the 23% uncertainty, except for C_4H_2, which is again about 35% lower than V1/IRIS.

In general, at 50°N we find in 2010 a return to the V1/IRIS values within the 35% uncertainty level for all molecules except the two complex hydrocarbons C_4H_2 and C_3H_4, which stay well below the 1980 abundances by about 50-55%. Again, the May 2010 50°N CIRS nadir data at 2.5 cm^{-1} are close to the high resolution values (differing by no more than ±15%) as also noted in Bampasidis et al. (2012) (compare the open and full circles on Fig. 3c for 2010 values).

We also considered ground-based and disk-averaged ISO data obtained before Cassini or more recently with Herschel (see Table 1). These data are limited to a few molecules and do not show, as far as we can see, any significant variations within a Titan year. Only the ISO data, taken toward the northern fall equinox (NFE, occurring in 1995), yield somewhat higher values for the species discussed here, such as HCN. One of the rare models dealing with long-term variations in Titan's atmosphere over a Titan year starting in 2000 (Hourdin et al. 2004, their Fig. 9), shows that soon after NFE, in the 80-240 km altitude range, the high-latitude HCN concentration grows very fast under the effect of downward advection, as do the latitudinal contrasts with low latitudes, reaching a maximum, so that the ISO disk-average data, which include some of the polar enhancement in gaseous components observed at NFE, may indeed exhibit higher values than any disk-resolved space equivalent data. However, it is very difficult to conclude that the ISO values are indeed higher than the V1/IRIS or the CIRS ones, given the impossibility to properly assess and compare ground-based or Earth-bound observations with space *in situ* ones given the differences in altitudes and regions probed, in spectral resolution, in modeling parameters, etc. We note, however, that the HCN stratospheric vertical profile obtained by Herschel/SPIRE recently (Courtin et al. 2011) for July 2010 is in good agreement with our findings at around 5 mbar (125 km in altitude) for equatorial latitudes (~1.5 10^{-7}, Fig. 3 in Bampasidis et al. 2012;

Fig. 5b and Table 2 of Coustenis et al. 2010), given that we only consider constant vertical profiles. We deplore, in general, the lack of more ground-based observations of Titan's atmospheric chemistry, which could provide good comparison points even on a disk-average level during a Titan year.

We also note that the results of a recent analysis of CIRS limb data (Vinatier et al., 2010) at 50°S, 1°N and 51°N data taken in June 2010, but covering higher altitudes (up to 500 km) and the simple vertical distributions of some hydrocarbons and nitriles retrieved from scarce horizontal viewing V1/IRIS data (Coustenis et al. 1991) are compatible in the general trend showing the nitriles increasing with altitude faster than the hydrocarbons. But again, the comparison cannot be pushed too far given the differences in vertical resolution, modeling, gaseous distributions, thermal structure, etc.

5. DISCUSSION

The fulfillment of one Titan year of observations provides us for the first time with the opportunity to evaluate the relative role of different physical processes in the long-term evolution of this complex environment. By comparing V1 (1980), ISO (1997) and Cassini (2010) data we find that the temperature structure is quite similar within error bars (Fig. 2). The chemistry also appears to be generally unchanging (V1/IRIS vs. Cassini/CIRS are within 25-35%), with some exceptions, among the more complex hydrocarbons such as C_3H_4 and C_4H_2.

The return of today's abundances to values close to the ones derived from Voyager spectra (at the same season) is an indication that, as for the Earth, the solar radiation dominates over other energy sources, even at 10AU. Nevertheless, the differences observed (lower C_3H_4 and C_4H_2 mixing ratios) and the slightly higher values observed from the ground and from ISO near the NFE could suggest that other processes may be at play as well, for example, the variability of the solar insolation itself through the 11-year solar cycle or complex circulation phenomena. We also note from the variations during the Cassini mission found for the gases investigated here, that in the South pole, some of the minor species tend to show a strong increase in 2012, in accordance with what is expected from seasonal models of

Titan, indicating that a reversal of the north-south asymmetry is on-setting, and confirming the trend seen at higher altitudes in CIRS limb data (Teanby et al. 2012).

The detection of long-term temporal variations of the atmospheric chemical composition and thermal structure informs us on the impact of different processes such as photochemistry and dynamics. The main energy source defining Titan's chemical composition is solar radiation, while energetic particles from Saturn's magnetosphere, as well as galactic cosmic rays have also a significant contribution. All these energy sources vary temporally in magnitude during the course of one Titan year. C_3H_4 and C_4H_2 are short-lived and low-abundance complex hydrocarbons in Titan’s stratosphere and hence more prone to inter-annual variations. The temporal and spatial (due to Titan's inclination) variations in the energy input to Titan's atmosphere is a driver for changes in the advection patterns, which in turn provide a stronger variability in the latitudinal abundances of photochemical species. Furthermore, both the changes in the energy field and on the dynamics affect the production and evolution of aerosols in Titan's atmosphere. The abundance peak corresponds to a period during which the observed collapse of the detached aerosol layer (West et al. 2011) suggests that the dynamics went through a rapid transition which should influence the gas distribution and can be tied to the atmospheric circulation reversal predicted by GCM numerical models (Hourdin et al. 2004; Rannou et al. 2005; Crespin et al. 2008; Lebonnois et al. 2012). At the same time, the variable north/south asymmetry in Titan's albedo and haze content reveals the consequences of seasonal changes in the aerosol properties deeper in the atmosphere (Jennings et al. 2012).

Circulation and photochemical models must satisfy the constraints set by these new results, and further observational constraints will come from data acquired during the Cassini mission and up until the next summer solstice (2017). We note that we are still lacking disk-resolved data of the atmospheric composition for seasons from summer to winter solstice in the northern hemisphere.

Acknowledgments : We thank Florence Henry, Marcia Segura and Nicolas Gorius for help with the data during this project. We are grateful to Pascal Rannou and Sebastien Lebonnois for discussions on GCM models. The authors acknowledge the support of the ESA/NASA Cassini mission funds through the CNES program. AC has received support from the Agence Nationale de la Recherche (ANR projects "APOSTIC" #11BS56002, France). NAT received support from the UK Science and Technology Facilities Council and the Leverhulme Trust. Support for GO was provided by NASA to the Jet Propulsion Laboratory, California Institute of Technology.

REFERENCES

Achterberg, R. K., Conrath, B. J., Gierasch, P. J., Flasar, F. M., & Nixon, C. A. 2008, Icarus, 194, 263
Achterberg, R. K., Gierasch, P. J., Conrath, B. J., Flasar, F. M., & Nixon, C. A. 2011, Icarus, 211, 686
Bampasidis, G., Coustenis, A., Achterberg, R. K., et al. 2012, ApJ, 760, 144
Courtin, R., Swinyard, B. M., Moreno, R., et al, P. 2011, Astron. & Astrophys., 536(L2)
Coustenis, A. & Bézard, B. 1995, Icarus, 115, 126
Coustenis, A., Bezard, B., Gautier, D., Marten, A. & Samuelson, R. 1991, Icarus 89, 152-167
Coustenis, A. et al. 2003, Icarus 161, 383-403
Coustenis, A., Achterberg, R., Conrath, B., et al. 2007 Icarus, 189, 35
Coustenis, A. et al. 2008, Icarus 197, 539-548
Coustenis, A., Jennings, D. E., Nixon, C. A., et al. 2010, Icarus, 207, 461
Crespin, A. et al. 2008, Icarus 197, 556–571
Flasar, F. M., Kunde, V. G., Abbas, M. M., et al. 2004, Space Sci. Rev., 115, 169
Flasar, F. M., Achterberg, R. K., Conrath, B. J., et al. 2005, Science, 308, 975
Gillett, F. C. 1975, ApJ, 201, L41
Gurwell, M. A. 2004, ApJL, 616, L7
Hanel, R., Crosby, D., Herath, L., et al. 1980, Appl. Optics, 19, 1391
Hidayat, T., Marten, A., Bezard, B., et al. 1997, Icarus, 126, 170
Hourdin, F., Lebonnois, S., Luz, D. & Rannou, P. 2004, J. Geophys. Res. 109
Jacquinet-Husson, N., Crepeau, L., Armante, R., et al. 2011, JQSRT, 112, 2395
Jennings, D. E., Nixon, C. A., Jolly, A., et al. 2008, ApJL, 681, L109
Jennings, D. E., et al. 2012, ApJL, 761, L15
Kim, S. J., Geballe, T. R., Noll, K. S. & Courtin, R. 2005, Icarus, 173, 522
Kostiuk, T., Fast, K., Livengood, T. A., et al. 1997, Planetary and Space Science, 45, 931
Kostiuk, T., Livengood, T. A., Hewagama, T., et al. 2005, Geophys. Res. Lett., 32, 22205
Kostiuk, T., Hewagama, T., Fast, K. E., et al. 2010, Plan. Space Sci., 58, 1715
Lebonnois, S., Burgalat, J., Rannou, P. & Charnay, B. 2012, Icarus 218, 707–722
Letourneur, B. & Coustenis, A. 1993, Planet. Space Sci. 41, 593-602
Livengood, T. A., Hewagama, T., Kostiuk, T., Fast, K. E., Goldstein, J. J. 2002, Icarus, 157, 249
Livengood, T. A., Kostiuk, T., Sonnabend, G., et al. 2006. J Geophys. Res (Planets), 111.
Marten, A., Hidayat, T., Biraud, Y., Moreno, R. 2002. Icarus, 158, 532-544..

Niemann, H. B., Atreya, S. K., Demick, J. E., et al. 2010, J. Geophys. Res., 115, E12006
Nixon, C. A., Achterberg, R. K., Vinatier, S., et al. 2008a, Icarus, 195, 778
Nixon, C. A., Jennings, D. E., Bézard, B., et al. 2008b, ApJL, 681, L101
Nixon, C. A. et al. 2009, Planet. Space Sci. 57, 1573-1585
Orton, G. 1992, ESA Symposium on Titan (SEE N92-32348 23-91).
Rannou, P., Lebonnois, S., Hourdin, F., Luz, D., 2005, Adv. Space Res., 36, 2194
Roe, H. G., Greathouse, T. K., Richter, M. J. & Lacy, J. H. 2003, The Astrophysical Journal Letters, 597, L65-L68.
Rothman, L. S., Gordon, I. E., Barbe, A., et al. 2009, JQSRT, 110, 533
Tanguy, L., Bezard, B., Marten, A., et al. 1990, Icarus, 85, 43
Teanby, N. A., Irwin, P. G. J., de Kok, R., et al. 2008, Icarus, 193, 595
Teanby, N. A., Irwin, P. G. J., de Kok, R., et al. 2009, Phil. Trans. R. Soc. A, 367, 697
Teanby, N. A., Irwin, P. G. J., de Kok, R., Nixon, C. A. 2010, ApJL, 724, L84
Teanby, N. A., Irwin, P. G. J., Nixon, C. A., et al. 2012, Nature, 491, 732
Turtle, E. P., Perry, J. E., Hayes, A. G., et al. 2011. Science, 331, 1414
Vinatier, S., Bézard, B., Fouchet, T., et al. 2007, Icarus, 188, 120
Vinatier, S., Bézard, B., Nixon, C. A., et al. 2010a, Icarus, 205, 559
Vinatier, S. et al. 2010b, Icarus 210, 852
West, R.A., Balloch, J., Dumont, P., et al. 2011, Geophys. Res. Lett., 38, L06204

TABLES

Species	Observ. Date	Ls	Abundance	Altitude (Km)	Latitude	Observatory/ Instrument	Reference	Resolving Power	Range (cm^{-1})
C_2H_2	10 Jan 1997	194	$4.92 \pm 0.43 \times 10^{-6}$	stratosphere	disk average	ISO/SWS	Coustenis et al. 2003	1650-2000	330-1420
	21/11/2001	257	$7.00 \pm 4.50 \times 10^{-6}$	300	disk average	KECK 2 /NIRSPEC	Kim et al. 2005	2.5×10^{4}	3225-3472
			$5.60 \pm 3.30 \times 10^{-6}$	200					
			$4.00 \pm 2.30 \times 10^{-6}$	100					
C_2H_4	04/1974-04/1975	282-295	$1.10 \pm 0.90 \times 10^{-7}$	stratosphere	disk average	KPNO?	Gillett, 1975 & Orton, 1992	2.0×10^{-2}	Near-IR
	10 Jan 1997	194	$8.48 \pm 1.00 \times 10^{-8}$	stratosphere	disk average	ISO/SWS	Coustenis et al. 2003	1650-2000	330-1420
C_4H_2	10 Jan 1997	194	$1.67 \pm 0.42 \times 10^{-9}$	stratosphere	disk average	ISO/SWS	Coustenis et al. 2003	1650-2000	330-1420
	21 Nov 2001	257	$< 1.00 \times 10^{-7}$	stratosphere	disk average	KECK 2 /NIRSPEC	Kim et al. 2005	2.5×10^{4}	3225-3472
C_2H_6	04/1974-04/1975	282-295	$1.00 \pm 0.30 \times 10^{-5}$	stratosphere	disk average	KPNO/?	Gillett, 1975 & Orton, 1992	2.0×10^{-2}	Near-IR
	08/1993	153	$1.96 \pm 2.42 \times 10^{-5}$	stratosphere	center	IRTF/IRHS	Livengood et al. 2002	1.0×10^{6}	841-851
			$5.80 \pm 3.30 \times 10^{-6}$	stratosphere	west				
	10/1995	179	$9.40 \pm 9.40 \times 10^{-6}$	120 - 300	disk average	IRTF/IRHS	Kostiuk et al. 1997	1.0×10^{6}	841-851
	10/1995	179	$1.17 \pm 0.44 \times 10^{-5}$	stratosphere	east	IRTF/IRHS	Livengood et al. 2002	1.0×10^{6}	841-851
			$1.36 \pm 0.71 \times 10^{-5}$	stratosphere	west				

Species	Observ. Date	Ls	Abundance	Altitude (Km)	Latitude	Observatory/ Instrument	Reference	Resolving Power	Range (cm^{-1})
	09/1996	190	$1.60 \pm 0.77 \times 10^{-5}$	stratosphere	east	IRTF/IRHS	Livengood et al. 2002	1.0×10^{6}	841-851
			$5.20 \pm 5.90 \times 10^{-6}$	stratosphere	west				
	08/1993 - 09/1996	153 - 190	$8.80 \pm 2.20 \times 10^{-6}$	stratosphere	disk average	IRTF/IRHS	Livengood et al. 2002	1.0×10^{6}	841-851
	10 Jan 1997	194	$1.12 \pm 0.45 \times 10^{-5}$	stratosphere	disk average	ISO/SWS	Coustenis et al. 2003	1650-2000	330-1420
	18 Dec 2003	286	$3.00 \pm 1.50 \times 10^{-6}$	stratosphere	15N-40S West	Subaru/HIPWA C	Kostiuk et al. 2005	$1\text{-}25 \times 10^{6}$	851
			$9.00 \pm 5.00 \times 10^{-6}$	stratosphere	5N-50S East				
			$8.00 \pm 3.00 \times 10^{-6}$	130 - 300	Simultaneo usly East & West				
	08/1993 - 12/2003	153 - 286	$8.60 \pm 3.00 \times 10^{-6}$	100-300 km	disk average	IRTF/IRHS & Subaru/HIPWA C	Kostiuk et al. 2010	1.0×10^{6}	851
	15 Jan 2005	300	$9.30 \pm 7.30 \times 10^{-6}$	250 - 316	disk center	Subaru /HIPWAC	Livengood et al. 2006	$1\text{-}25 \times 10^{6}$	851
			$8.20 \pm 2.10 \times 10^{-6}$						
			$9.70 \pm 4.90 \times 10^{-6}$						
C_3H_8	10 Jan 1997	194	$1.67 \pm 0.83 \times 10^{-7}$	stratosphere	disk average	ISO/SWS	Coustenis et al. 2003	1850	330-1420
	14 Dec 2002	272	$6.20 \pm 1.20 \times 10^{-7}$	90 – 250	disk average	IRTF / TEXES	Roe et al. 2003	1.0×10^{5}	748
HCN	8 Sept 1986 – 6 May 1987	76 - 84	$7.50 \pm 0.80 \times 10^{-8}$	100	disk average	IRAM	Tanguy et al 1990	78 kHz & 1MHz	2.95
			$3.30 \pm 0.90 \times 10^{-7}$	170					
			$6.20 \pm 2.10 \times 10^{-7}$	200					

Species	Observ. Date	Ls	Abundance	Altitude (Km)	Latitude	Observatory/ Instrument	Reference	Resolving Power	Range (cm^{-1})
			$5.20 \pm 6.60 \times 10^{-6}$	300					
	22 May 1995	174	$5.00 \pm 1.10 \times 10^{-8}$	100	disk average	IRAM	Hidayat et al. 1997	78 kHz & 1MHz	2950
			$1.50 \pm 0.50 \times 10^{-7}$	170					
			$3.50 \pm 1.10 \times 10^{-7}$	200					
	10 Jan 1997	194	$2.42 \pm 0.40 \times 10^{-7}$	stratosphere	disk average	ISO/SWS	Coustenis et al. 2003	1850	330-1420
	04/1996 and 12/1999	200 and 232	$4.00 \pm 2.00 \times 10^{-8}$	100	disk average	IRAM	Marten et al. 2002	78 kHz & 1MHz	2960 & 8620
			$2.10 \pm 0.80 \times 10^{-7}$	170					
			$4.50 \pm 1.50 \times 10^{-7}$	200					
			$5.20 \pm 1.60 \times 10^{-7}$	250					
			$5.80 \pm 2.00 \times 10^{-7}$	300					
			$6.60 \pm 2.00 \times 10^{-7}$	350					
			$7.50 \pm 2.50 \times 10^{-7}$	400					
			$8.00 \pm 2.50 \times 10^{-7}$	450					
	21 Nov 2001	257	$1.00 \pm 0.20 \times 10^{-7}$	200	disk average	KECK 2/ NIRSPEC	Kim et al. 2005	2.5×10^4	3225 - 3472
			$4.10 \pm 2.00 \times 10^{-7}$	300					
			$1.00 \pm 0.25 \times 10^{-6}$	400					
			$5.00 \pm 2.00 \times 10^{-6}$	500					
	1 Feb 2004	288	$3.00 \pm 1.00 \times 10^{-7}$	83	disk average	SMA	Gurwell 2004		11.5

Species	Observ. Date	Ls	Abundance	Altitude (Km)	Latitude	Observatory/ Instrument	Reference	Resolving Power	Range (cm^{-1})
			$4.00 \pm 2.00 \times 10^{-7}$	200					
			$5.00 \pm 5.00 \times 10^{-6}$	300					
	July 2010	11	$1.5\ 10^{-7}$	125	disk average	Herschel/SPIRE	Courtin et al. 2011	~375	20-52
C_3H_4	10 Jan 1997	194	$1.19 \pm 0.40 \times 10^{-8}$	stratosphere	disk average	ISO/SWS	Coustenis et al. 2003	1650-2000	330-1420
CO_2	10 Jan 1997	194	$1.82 \pm 0.18 \times 10^{-8}$	stratosphere	disk average	ISO/SWS	Coustenis et al. 2003	1650-2000	330-1420

Table 1: Ground-based and ISO SWS observations of Titan's stratospheric composition. These data provide information about the atmospheric composition of Titan during the interval between Voyager and Cassini/Huygens missions, but are not directly comparable to the conclusions derived from spatially resolved interplanetary spacecraft observations. Details of the observatory and instrument are provided in the corresponding references.

Molecule	50°S	7°N	50°N	ISO disk-average
C_2H_2	$2.25\pm0.45 \times 10^{-6}$	$2.62\pm0.4 \times 10^{-6}$	$3.35\pm1.0 \times 10^{-6}$	$4.95\pm0.5 \times 10^{-6}$
C_2H_4	$1.14\pm0.45 \times 10^{-7}$	$1.13\pm0.3 \times 10^{-7}$	$2.55 \pm1.22 \times 10^{-7}$	$9.33\pm0.4 \times 10^{-8}$
C_2H_6	$9.50\pm1.85 \times 10^{-6}$	$1.01\pm0.15 \times 10^{-5}$	$1.35 \pm0.34 \times 10^{-5}$	$1.32\pm0.5 \times 10^{-5}$
C_3H_4	$5.60\pm1.75 \times 10^{-9}$	$7.80\pm1.6 \times 10^{-9}$	$3.10 \pm0.93 \times 10^{-8}$	$1.44\pm0.4 \times 10^{-8}$
C_3H_8	$1.40\pm0.6 \times 10^{-6}$	$1.60\pm2.2 \times 10^{-6}$	$2.10\pm1.0 \times 10^{-6}$	$4.76\pm0.8 \times 10^{-7}$
C_4H_2	$1.30\pm0.35 \times 10^{-9}$	$1.57\pm0.4 \times 10^{-9}$	$1.10\pm0.4 \times 10^{-8}$	$2.09\pm0. \times 10^{-9}$
HCN	$7.50\pm2.2 \times 10^{-8}$	$2.03\pm0.4 \times 10^{-7}$	$7.00\pm2.7 \times 10^{-7}$	$2.97\pm0.4 \times 10^{-7}$
CO_2	$1.55\pm0.27 \times 10^{-8}$	$1.50\pm0.2 \times 10^{-8}$	$1.00\pm0.3 \times 10^{-8}$	$2.05\pm0.2 \times 10^{-8}$

Table 2. New values of V1/IRIS abundance retrievals at 50°S, equator and 50°N with 3-sigma error bars including both systematic and random uncertainties. The ISO values were also re-calculated with a temperature profile matching the emission observed in the CH_4 ν_4 band at 1304 cm^{-1} and the new spectroscopic data available for some molecules. The corresponding altitudes are the same as in Coustenis et al. (2003). The re-analysis of the V1/IRIS data allowed us to detect in them for the first time C_6H_6, HC_3N and C_2HD (see fit in Fig. 1), albeit given the low spectral resolution of the Voyager spectra, we were unable to derive accurate mixing ratios for these molecules and therefore they are excluded from this paper. The same pertains to C_3H_8 and C_2H_4 which similarly bear large uncertainties. The CIRS abundances from 2006 to 2013 are shown with respect to V1/IRIS in Fig. 3.

FIGURE CAPTIONS

Figure 1. Upper panel: fit of the V1/IRIS Nov. 1980 data of Titan taken at 50°N, with the updated code and spectroscopic parameters. The spectral resolution is 4.8 cm^{-1}. The improved fit in the region 670-700 cm^{-1}, with respect to the Coustenis and Bézard (1995) publication, is due to the inclusion of the C_2HD and C_6H_6 bands which were not identified at that time. Lower panel: fit of the 0.5 cm^{-1} resolution CIRS spectrum taken in Jan. 2010. Left: FP3 region; right : FP4 region.

Figure 2. Retrieved thermal profiles from CIRS and V1/IRIS data (in full and dashed lines respectively) at 50°S, 50°N and equator for the 2010 nadir data and IRIS 1980 data. The CIRS temperature profiles correspond to April, July and January 2010 at 50°S, equator and 51°N respectively. The temperature profile corresponding to the ISO disk-averaged SWS data of 1997 is also shown in dotted black lines. The pressure/altitude ranges probed by these profiles vary with latitude, but are generally in the 0.1-10 mbar region (see text). The uncertainty is about 1 K at 1 mbar and 5 K at 5 mbar for the CIRS profiles and about 1 K more at each level for the IRIS profiles due to the higher noise. For ISO, the error bars are about 2 K at pressures lower than 1 mbar and at most 5 K at higher ones (altitudes lower than 200 km).

Figure 3 a) variations of the abundances of gases in Titan's stratosphere with respect to the V1/IRIS values at 50°S (normalized as 1) for: C_2H_2 (black), C_2H_6 (red), CO_2 (brown), HCN (blue), C_3H_4 (green), C_4H_2 (magenta). The arrows indicate the date of the 1980 V1 encounter. Larger open circles correspond to medium-resolution (2.5 cm^{-1}) data that we have in 2010. b) : same as a) but for the equator. c) : same as a) but for 50°N. The vertical error bars are only from CIRS relative uncertainties (see text). In mid-2010, at the time of the return to the Voyager encounter epoch (indicated by arrows), all gases show values within the uncertainty levels of 27%, 23% and 35% for 50°S, equator and 50°N, respectively (not shown in the figure to avoid confusion), which take into account the V1/IRIS errors also. Exceptions are C_3H_4 and C_4H_2 in some cases (see text).

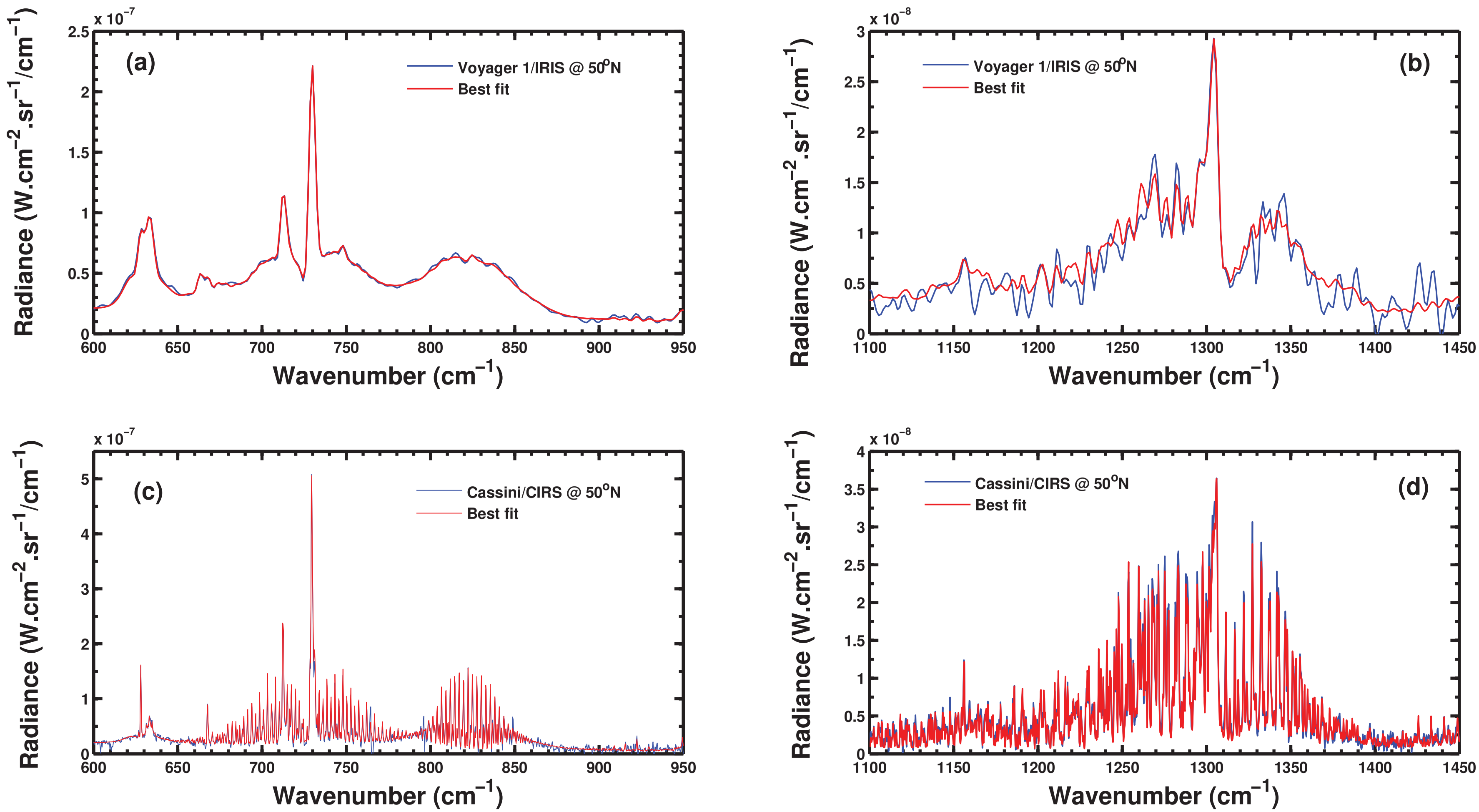
(a)
Voyager 1/IRIS @ 50°N
Best fit
Radiance (W.cm⁻².sr⁻¹/cm⁻¹)
x 10⁻⁷
Wavenumber (cm⁻¹)
(b)
Voyager 1/IRIS @ 50°N
Best fit
x 10⁻⁸
(c)
Cassini/CIRS @ 50°N
Best fit
(d)
Cassini/CIRS @ 50°N
Best fit

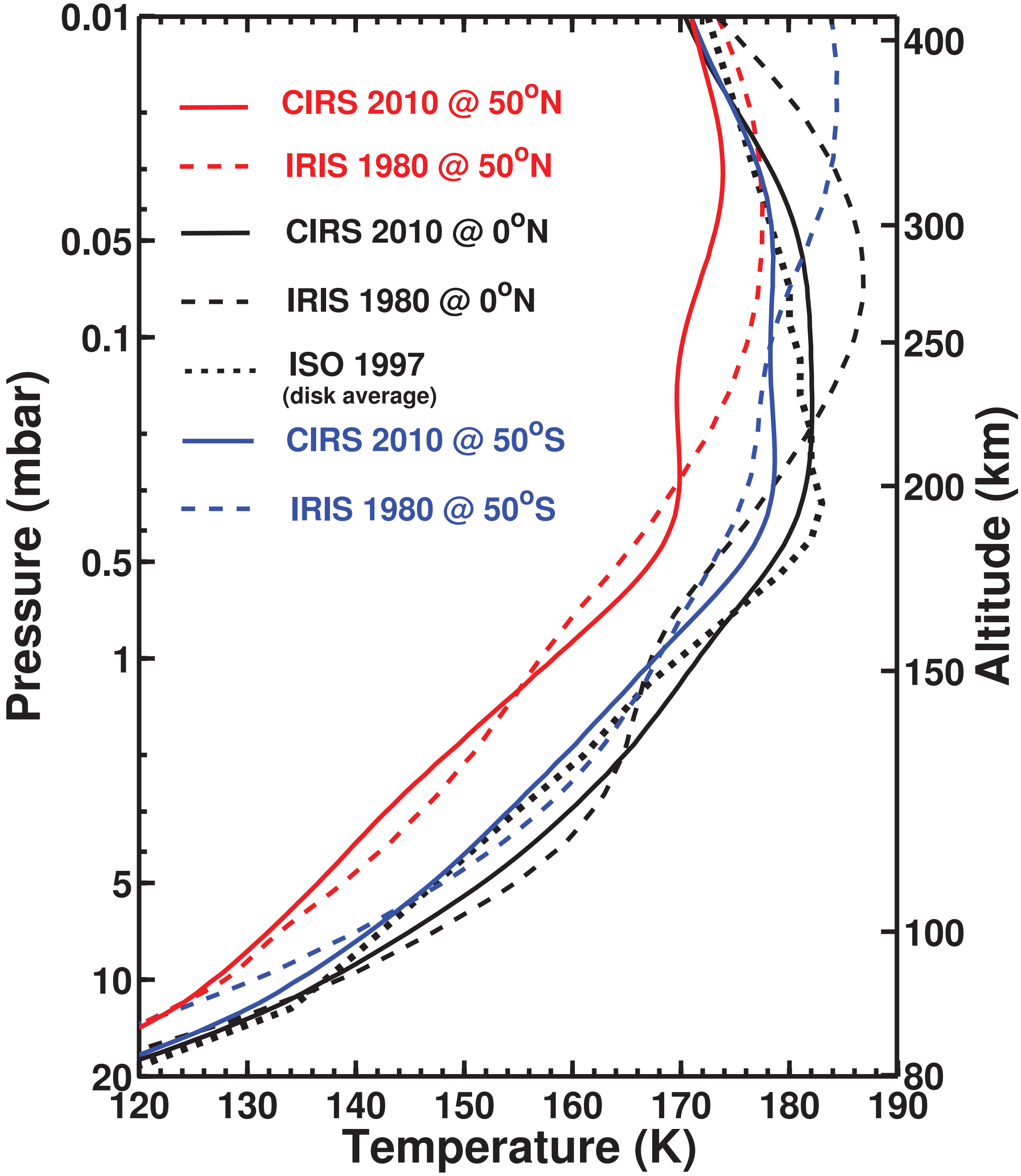

CIRS 2010 @ 50°N
IRIS 1980 @ 50°N
CIRS 2010 @ 0°N
IRIS 1980 @ 0°N
ISO 1997
(disk average)
CIRS 2010 @ 50°S
IRIS 1980 @ 50°S
Pressure (mbar)
0.01
0.05
0.1
0.5
1
5
10
20
Altitude (km)
400
300
250
200
150
100
80
120
130
140
150
160
170
180
190
Temperature (K)

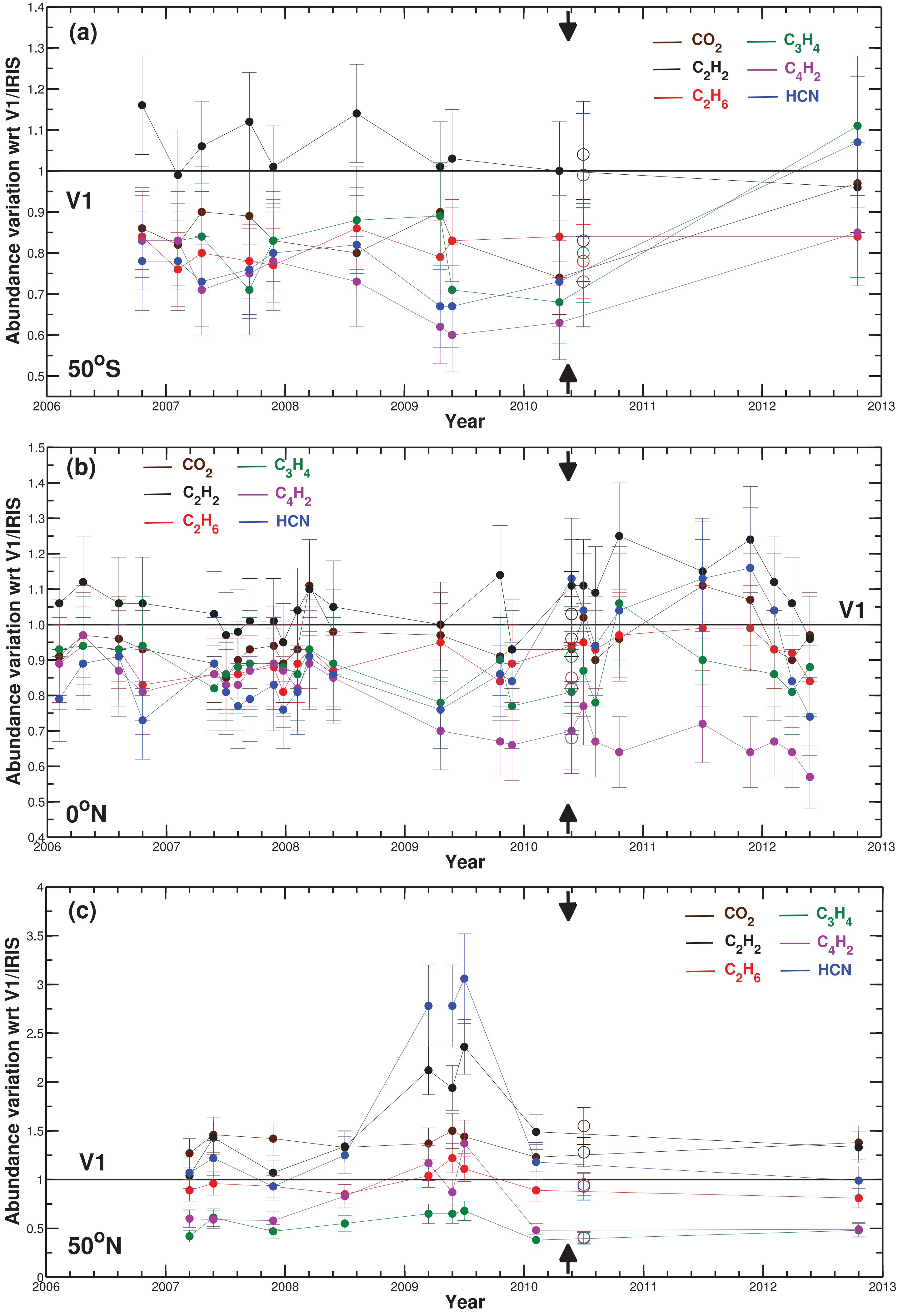
(a)
CO_2
C_2H_2
C_2H_6
C_3H_4
C_4H_2
HCN
V1
50°S
Abundance variation wrt V1/IRIS
Year
(b)
V1
0°N
(c)
V1
50°N